USE OF GRID REINFORCEMENT IN HMA OVERLAYS - A TEXAS FIELD CASE STUDY OF HIGHWAY US 59 IN ATLANTA DISTRICT

Lubinda F. WALUBITA[1], Enad MAHMOUD[2], Sang ICK LEE[1], Gisel CARRASCO[2], Julius J. KOMBA[3],
Luis FUENTES[4*], & Tito P. NYAMUHOKYA[1]

Abstract: One of the common methods to mitigate reflective cracking, in existing cracked pavements, is the use of interlayer grid reinforcements in hot-mix asphalt (HMA) overlay construction during maintenance and/or rehabilitation projects. As a means of sharing the practical experience, lessons learned, and demonstrating the performance benefits of using interlayer grid-reinforcements, this paper presents a field case study where different types of grid reinforcements (namely geosynthetic paving mats) were used in HMA overlay construction to mitigate reflective cracking and thereafter, field performance was monitored and evaluated periodically. Two HMA overlay test sections (denoted as Sec13 and Sec14), reinforced with different geosynthetic materials were constructed in 2011 over an existing cracked HMA pavement (with transverse cracks) on an in-service highway US 59 in the Atlanta District of Texas. Field performance was subsequently monitored/evaluated for a period of over seven years against an adjacent Control section (Sec01), without grid reinforcement, on the same US 59 highway. Under the same pavement structure, traffic loading, and climatic conditions, various performance indices were evaluated semi-annually including reflective cracking, rutting, longitudinal surface profiles, and interlayer bonding. While the rutting performance was indifferent on all the three test sections after 7 years of service, 17% of reflective cracking was measured on the Control section versus 4% on the grid-reinforced test sections – demonstrating that the use of grid reinforcement (i.e., geosynthetic paving mats) has been effective in mitigating reflective cracking from the existing cracked HMA pavement. Similarly, while coring indicated satisfactory interlayer bonding conditions on all the three test sections, the rate of pavement surface roughness deterioration was also hardly different on all the three test sections – albeit that the Control section (Sec01) exhibited superiority in terms of the profile indices (smoothness/serviceability) than the grid-reinforced test sections (Sec13 and Sec14).

Keywords: HMA, Overlay, Reflective cracking, Grid-reinforcement, Geosynthetic, Paving-mat

---

**Corresponding Author* | lfuentes@uninorte.edu.co
[1] Texas A&M Transportation Institute (TTI), The Texas A&M University System, College Station, TX, USA
[2] Texas Department of Transportation (TxDOT), Austin, TX, USA
[3] University of Pretoria/CSIR – Council for Scientific and Industrial Research, Pretoria, South Africa
[4] Department of Civil and Environmental Engineering, Universidad del Norte, Barranquilla, Colombia

INTRODUCTION

One of the critical structural distresses occurring in hot-mix asphalt (HMA) overlays over flexible and rigid (concrete) pavements is reflective cracking – often costing highway agencies millions of taxpayers' dollars in maintenance and rehabilitation (*M&R*) activities, particularly with the occurrence of other secondary defects such as water ingress through the cracks and subsequent damage to the underlying sub-structure. As exemplified in Fig. 1, various methods including application of crack-impeding and interlayer grid-reinforcements are often used to mitigate reflective cracking in existing cracked pavements used in *M&R* projects during HMA overlay construction [1-8].

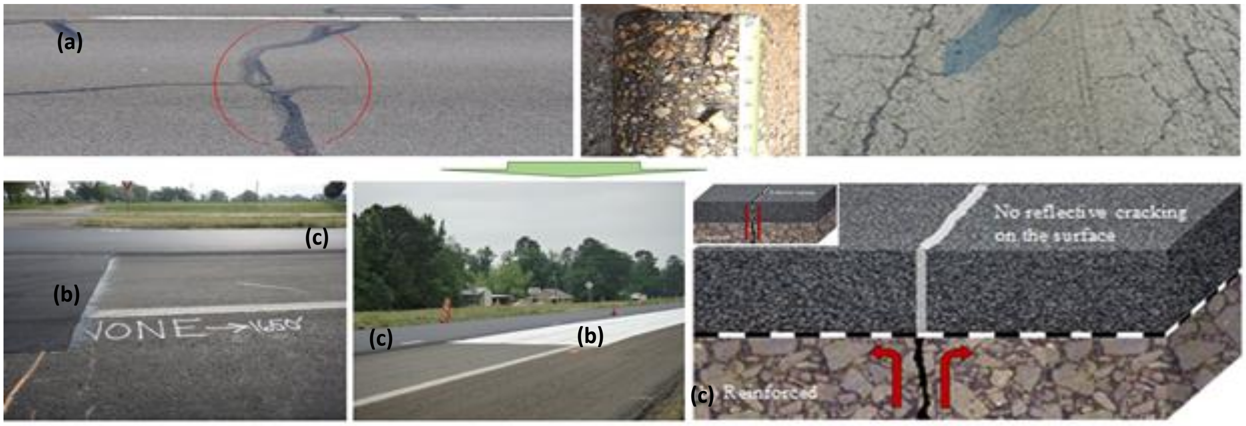

Fig. 1. (a) Old Cracked Pavement, (b) Grid-Reinforcement, and (c) Overlay Construction.

From Fig. 1, it is clearly evident that the primary structural function of the interlayer grid-reinforcement is to mitigate and retard the upward propagation of cracks from an existing cracked pavement to the HMA overlaid surface. The grid-reinforcement aids in prolonging the cracking (reflective) resistance, longevity, and service life of the pavement. In some cases, the grid-reinforcement also serves as a waterproofing membrane for the sub-structure.

In 2010, the Texas Department of Transportation (TxDOT) initiated a research study to develop, manage, and maintain a long-term "Microsoft Access® database for Texas flexible pavements and overlays", namely the Texas Data Storage System (DSS) [9]. As of to date, the DSS comprises of 115 in-service highway test sections with substantial data, related to material properties and performance, that has been routinely collected since 2010; consisting of design, construction, layer material properties (laboratory/field measured), traffic, climate, and field performance data. Three overlay test sections (two grid-reinforced and one unreinforced) on in-service highway US 59, from the DSS, are the subject of this paper.

As an extract from the DSS, this paper presents highway US 59 (in the Atlanta District of Texas) as an in-service field case study to demonstrate and share the practical experiences, lessons learned, and performance benefits of using grid reinforcements in HMA overlays; with particular emphasis on reflective crack mitigation, rutting, surface roughness/texture, and interlayer bonding [9]. With the use of grid reinforcements, interlay bonding often becomes an issue of concern and hence, this aspect is also considered in this paper. An adjacent Control (un-reinforced) section on the same in-service highway (US 59) was used as the reference datum to substantiate the merits/demerits of using grid reinforcements in HMA overlays.

In the subsequent sections, a literature review is presented followed by the highway US 59 test sections, grid reinforcements, and HMA overlay construction details. The experimental plan for the study is subsequently presented followed by the field-performance test results, analysis, and synthesis of the findings. The paper then concludes with a summary of key findings and recommendations.

LITERATURE REVIEW

Various interlayer grid-reinforcement materials including geogrids, geotextiles, geosynthetics, paving-mats, paving fibers, fiberglass, polyester-based, etc., are presently available on the commercial market and widely used in HMA overlays during M&R activities [8,10]. The grid reinforcements are typically provided in HMA overlays to mitigate reflective cracking and extend the service life of the overlaid pavements. World-wide, numerous literature publications have reported over 10% improvement and extension in the overlay service life with the use of grid reinforcements. Colbond [11], for instance, reported a performance improvement of about 1.1 to 1.3 times in comparison to un-reinforced control sections. Expressed in terms of the HMA overlay crack life extension, AG [2] and Fyfe [5] have reported 2.0 to 3.0 times improvement. Similarly, 2.0 to 3.0 times improvement in overlay life has been reported in the Delft and Nottingham studies [7]. In general, most of the literature reviewed has reported a performance benefit ratio of 1.1 to 6.0 times based on a summation of multiple studies and field performance observations and predictions [1-8,11]. However, some studies have also reported little to no performance improvement or appreciable benefits with the use of grid-reinforcements in HMA overlays [12-14]. Overall, while some studies [12-14] have reported no appreciable performance improvements, there is no doubt that most of the literature reviewed has provided some insights into the potential benefits of using grid-reinforcements in HMA overlays to mitigate reflective cracking and extend the longevity of the entire pavement structure. As an extract from the DSS, the case study presented in this paper exemplifies one of Texas' field experience and practical lessons learned with the use of grid reinforced HMA overlays as a *M&R* option [9]. In the paper, the performance benefits of grid reinforcement in HMA overlays, expressed in terms of the grid efficiency factor (*GEF*), was also assessed with a focus on reflective crack mitigation.

Unlike reflective cracking and rutting, the particular literature reviewed is limited as regards to the impacts of grid reinforcement on the pavement surface roughness/smoothness, texture/friction, and serviceability of the HMA overlays. That is, most of the reviewed literature is focused mainly on the reflective crack-resistance performance of the grid-reinforced HMA overlays [1-8]. By contrast, this field case study provides a holistic assessment incorporating all these performance aspects including periodic ground-penetrating radar (GPR) and falling-weight deflectometer (FWD) testing for forensic/subsurface defects and strength (modulus/stiffness) characterization as a function of time.

Interlayer bonding is often an issue of concern when grid reinforcements are used in HMA overlays. By default, there is a theoretical notion that the application of grid reinforcements inherently reduces and weakens the interlayer bonding strength of the HMA overlay, which may not be the case. However, most of the literature reviewed provided shear-bond strength data on un-reinforced HMA overlays, mostly based on laboratory prepared-samples [15-29]. Based on field core testing, Wilson et al [17] measured a shear-bond strength range of 15-95 psi with satisfactory in-service (field) interlayer bonding performance [11]. From testing both field cores and laboratory prepared-samples with different grid-reinforcement materials, Walubita et al [15] recorded interlayer shear-bond strengths varying from 33 to 175 psi. Overall, shear-bond strength values ranging from as low as 15 psi to as high as 217 psi were reviewed in the literature, mostly for un-reinforced HMA and subjected to varying laboratory test methods/conditions [15-29]. Furthermore, different institutions, states, and countries seem to have different criteria for characterizing and quantifying the interlayer bond strength in HMA; ranging from a tolerable 40 psi [17] to a more stringent shear-bond strength value of 100 psi [18,19]. As discussed subsequently in this paper, the aspect of interlayer bonding was also addressed in this case study through coring from both the Control and grid-reinforced test sections followed by laboratory shear-bond strength testing.

In addition to proper grid material selection, proper grid installation, good construction practices, and stringent quality assurance and quality control (QA/QC) protocols are imperative to realize the full benefits of using grid-reinforcements in HMA overlays. All these aspects are also addressed and discussed in this paper. Note that in this paper, the word “grid” was interchangeably used to refer to “geosynthetic/paving-mats”.

THE US 59 HIGHWAY CASE STUDY

The overlay test sections on highway US 59, in the Atlanta District of Texas, are an integral part of the ongoing DSS project for Texas flexible pavements and overlays [9]. As presented and discussed in this paper, the DSS test sections on highway US 59 comprises of the following three in-service overlay sections:

a) Section 01 = un-reinforced control section, designated as Sec01 in the DSS.
b) Section 13 = fiberglass/polyester-based (F/B) reinforced section, designated as Sec13 in the DSS.
c) Section 14 = polypropylene-based (PP) reinforced section, designated as Sec14 in the DSS.

Each of the three overlay test sections is 720 ft long by 12 ft wide, located in the outside lane of US 59, southbound (SB) direction, between reference markers (RM) 308 and 310, north of the City of Carthage, Texas. The test section location, plan view, and pavement structure details are shown in Fig. 2.

#	Layer	Thickness (Inches)	Year Constructed
4	HMA overlay (Type D = 5.1% PG64-22 with 20% RAP)	2.0	2011
3	Interlayer grid-reinforcement ⇒ **None** for Sec01, **F/B** for Sec13, & **PP** for Sec14		2011
2	Existing HMA	~ 11.5	-
1	Base (lime fly-ash [LFA] treated)	~ 16.0	-
0	Subgrade	∞	-

Fig. 2. US 59 Test Section Location, Plan View, and Pavement Structure.

As documented elsewhere [9], the 11.5 inches thick existing HMA in Fig. 2 comprise of dense-graded HMA mixes, 5/8" nominal maximum aggregate size (NMAS) with about 4.4 to 4.7% PG 70-22 asphalt-binder and limestone/quartzite aggregates. The 16 inches thick LFA treated base layer comprise of about 20 lb/sy lime and 40 lb/sy fly-ash in a dry application.

US 59 Pavement Prior to HMA Overlay Construction

As part of the TxDOT routine road maintenance programme, highway US 59 needed an overlay because of, among other distresses, crack manifestation that included transverse, longitudinal, and alligator cracking, both top-down and bottom-up initiated (based on coring). A pre-construction distress survey and field testing of the existing cracked HMA pavement was conducted to measure and document the existing distresses prior to placement of the interlayers grids and HMA overlay construction. The pre-construction walking survey comprised of manually counting the number of cracks and measuring the crack length and width, location of the cracks (both longitudinally from start of the test section and transversely from outside lane edge), identifying crack type (i.e., transverse, alligator, longitudinal, etc), and taking pictures of the pavement surface. Fig. 3 shows the surface condition of highway US 59 and an example of a crack-mapping survey conducted in 2011 before the HMA overlay construction.

Fig. 3a. Existing Highway US 59 Pavement Condition Prior to HMA Overlay Construction.

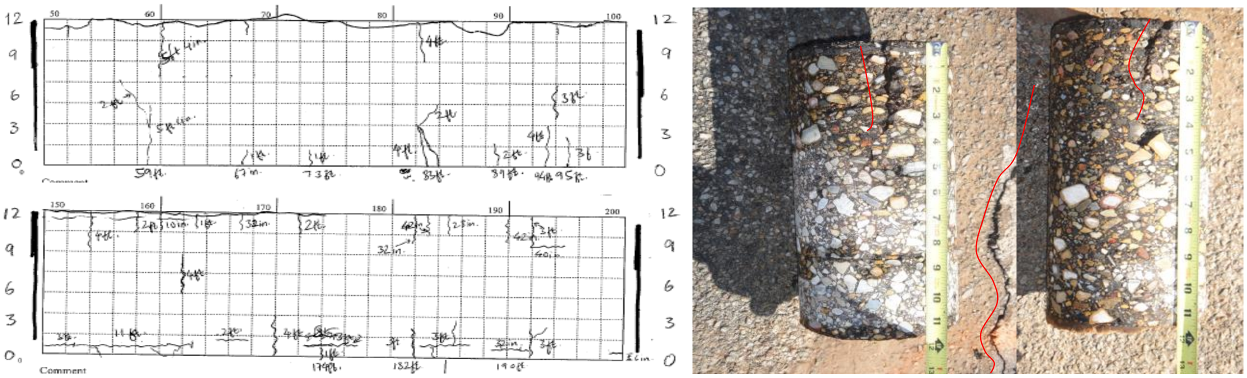

Fig. 3b. Example Pre-Construction Crack-Mapping (Walking) Survey on US 59.

As shown in Fig. 3(b), some of the pre-construction field-testing included coring samples to assess the degree of crack depth and quantify the existing pavement layer thicknesses. As catalogued in the DSS (*11*), other tests included GPR for subsurface condition assessment and existing pavement layer thickness determination, rutting, FWD testing for HMA modulus and pavement strength characterization, and dynamic cone penetration (DCP) testing for base/subgrade modulus, strength, and thickness characterization.

Grid Reinforcement Materials

For the purposes of impartiality and considering that grid materials are commercial products, only generic names (with no index properties) are given in this paper. The grid materials used on US 59 were all geosynthetic paving mats, namely a fiberglass/polyester-based paving mat (denoted herein as F/B) on Sec13. Its ASTM D 7239 generic term is hybrid geosynthetic paving mat [30]. The geosynthetic material used on Sec14 is a non-woven needle punched polypropylene-based paving mat (denoted herein as PP).

Grid Reinforcement and HMA Overlay Construction

As shown in Fig. 4, the construction process comprised of tack-coat application, geosynthetic installation (in the case of test sections Sec13 and Sec14), HMA overlay placement, and compaction thereafter, which was monitored, recorded, and documented for cataloguing in the DSS [9]. The HMA overlay mix is a standard Texas 12.5-mm nominal maximum aggregate size (NMAS) fine-graded Type D surfacing mix comprising of 5.1% PG 64-22 asphalt-binder with quartzite aggregates and 20.1% recycled asphalt pavement (RAP) material – compacted to a 2-inch thickness at a target density of 97%.

Fig. 4. Geosynthetic Installation and HMA Overlay Construction.

The construction operation, in a line-sequence, comprised of a tack-coat sprayer (0.085 gal/sy PG 64-22 application rate), a grid installation equipment, dump trucks, material transfer device (Roadtec), a paver, and compactors. The compaction pattern comprised of 4 to 6 vibratory passes (2 rollers, 12.15 ton each) with a 200 lb joint roller. As catalogued in the DSS, QA/QC testing during and just after construction included the following: material sampling, temperatures, infrared thermal imaging (mat temperature), density (nuclear density gauge), compaction thickness and density (GPR), field coring for density measurements and extraction tests (asphalt-binder and aggregates), smoothness (surface profiles), and taking pictures [9]. As per TxDOT construction specifications, the QA/QC test requirements were satisfactorily met with the average air, pavement surface, and HMA mat temperatures being 84.6, 145.4, and 183.6 °F, respectively [9]. The compacted HMA mat thickness and density averaged 2.01 inches and 96.3%, respectively, with the effective core extracted asphalt-binder content being 5.2% [9]. However, minor dips (0.25 ft. width and 0.15 in. depth) were measured on the grid-reinforced test sections.

FIELD TEST PLAN AND PERFORMANCE MONITORING

Since geosynthetic installation and HMA overlay construction in 2011, the test sections have been periodically visited and monitored twice per year (just after summer to capture the high temperature-related distresses and just after winter to capture the low temperature related distresses), for routine performance testing (RPT) and distress measurements/evaluation. The field-testing schedule including pre-construction, during construction, and RPT is shown in Fig. 5 with the latest site visit being April 25, 2018.

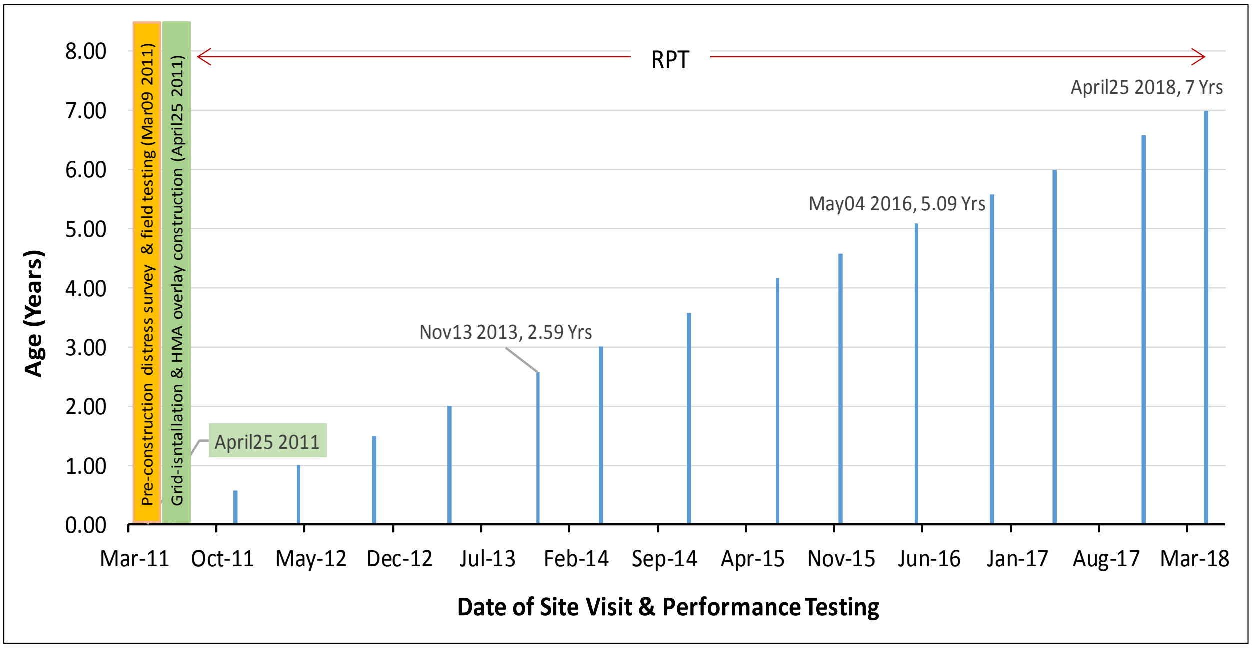

Fig. 5. RPT Field Plan and Schedule for the US 59 Overlay Test Sections.

Since overlay construction on April 25, 2011, Fig. 5 shows that the test sections clocked 7 years of service on April 25, 2018. Pre-construction distress surveys were conducted on March 9, 2011. In line with the ongoing database (DSS) project, the next site visit and RPT is tentatively scheduled for spring 2019.

As documented in the DSS and shown in Fig. 5, the RPT comprise of the following performance evaluations and field testing: GPR (subsurface defects); crack (walking) surveys/measurements; surface rut measurements (using a straightedge); raveling (aggregate loss); bleeding; temperature measurements (air and PVMNT); high-speed profiles and surface roughness (IRI and PSI); FWD (surface deflections, layer modulus, and pavement strength); DFT-CTMeter (friction characteristics and surface texture); coring (as needed); traffic measurements (volume counts and vehicle weights); taking pictures; etc. [9]. The respective field tests are listed in Table 1.

The traffic data are being measured/collected using pneumatic traffic tube (PTT) counters and portable weigh-in-motion (WIM) systems to obtain the volume counts, vehicle speed, vehicle classification, vehicle weights, and load spectra data including ADT, ADTT, percentage trucks, 18-kip ESALs, etc. Note that the reference limit/criteria for the performance evaluation indicators such as rutting, cracking, surface, and serviceability index were based on the TxDOT Pavement Management Information System (PMIS), TxDOT pavement manual, Texas Mechanistic-Empirical pavement design system (TxME), the Federal Highway Authority (FHWA)'s pavement condition criteria, the Mechanistic-Empirical Pavement Design Guide (M-E PDG) manual of practice [9].

Table 1 RPT Field Tests and Data Characteristics.

#	Test	Test Procedure	Output Data
1	Cracking	Visual walking surveys • Alligator cracking • Block cracking • Transverse cracking • Longitudinal cracking	• Crack length/width • # of cracks • % of cracking • Severity
2	Surface rutting	Straightedge at 100-ft interval in both wheel paths	Surface rut depth (in.)
3	Other distresses	Visual walking surveys • Raveling (aggregate loss) • Bleeding, patching, etc	• Severity • % coverage
4	Temperatures	Temperature measurements	• Air • Pavement surface • At 1-inch pavement depth
5	Surface profiles	High-speed profiler in both wheel paths	• Surface roughness & serviceability index – IRI – PSI
6	FWD	9 kips drop every 25-ft in outside wheel path	• Surface deflections • Back-calculated modulus (measure of pavement strength) • Load transfer efficient (LTE)
7	GPR	Outside wheel path	• Layer thickness • Forensic defects
8	DFT & CTMeter	Minimum 3 points as follows: • 1 in shoulder • 2 in inside wheel path	• Texture & friction characteristics • DFT – microtexture • CTMeter - macrotexture • Predicted IFI • Predicted SN
9	Coring	6-inch diameter cores, both in & outside wheel paths	• Visual interlayer bonding assessment • Subsurface defect assessment • Laboratory testing of cores including: – Interlay shear-bond strength – Modulus & stiffness – Rutting (HWTT) & cracking (IDT/OT) – Aging (asphalt-binder extraction tests)
10	Pictures	Taking pictures	• Foreground view & critical distresses

11	Traffic	Traffic data collection by • Pneumatic traffic-tube (PTT) counters • Portable WIM	• Traffic volume & classification – ADT, ADTT & %Truck – Vehicle class distribution (VCD) – Vehicle speed – Traffic growth rate (G_r) • Vehicle weights & axle load spectra – GVW – Axle load distribution – 18-kip ESALs

Legend: ADT = average daily traffic, ADTT = average daily truck traffic, CTM = circular texture meter, DFT = dynamic friction tester, GVW = gross vehicle weight, ESAL = equivalent single axle load, HWTT = Hamburg wheel tracking test, IDT = Indirect tension test, IFI = international friction index, OT = Overlay tester, SN = skid number, WIM = weigh-in-motion

FIELD PERFORMANCE, TEST RESULTS, AND ANALYSIS

As listed in Table 1, various field performance tests ranging from visual distress observations to FWD are being routinely (twice per year) conducted on the test sections, spanning a 7-year performance-monitoring period as of April 25, 2018 [9]. However, as presented and discussed in the subsequent text, the primary focus of this paper is on the following indicators: traffic, temperature, surface rutting, cracking, surface profiles, interlay bonding, and pavement surface condition.

Traffic and Temperature Measurements

As periodically measured using the pneumatic traffic-tube (PTT) counters and portable WIM, all the three test sections endured virtually the same level of traffic loading over the 7-year period. The overall average traffic comprised of an ADT of 4,208; 38% trucks (ADTT = 1,599); and 2,612 daily 18-kip ESALs [9]. The overall average truck speed was 66.5 mph while the designated speed limit for US 59 at the test section site is 75 mph. Temperatures were also periodically measured during RPT for the air, pavement surface, and at a 1-inch depth below the surface at the mid-depth of the overlay to characterize and quantify the true temperature of the HMA for effective response and distress evaluation. On average, the temperature varied between 120°F (summer) and 40°F (winter), which is not uncommon in the Texas wet-dry (WC) climatic region where the test sections are located i.e., Panola County of Atlanta District (Texas). The maximum (summer) and minimum (winter) recorded temperatures at 1-inch pavement depth were 145 and 25°F, respectively.

Pavement Surface Rutting Performance

Fig. 6 shows that the surface rutting performance of the three test sections are indifferent and well below TxDOT PMIS' 0.50 inches rutting criteria; with Sec13 (0.20 inches) on the slightly higher side and Sec14 (0.17 inches) on the lower side [9]. For the same traffic level, temperature conditions, and pavement structure, the performance results in Fig. 6 infers that the interlayer grid-reinforcements, namely F/P and PP, had no major structural impact on the rutting performance of the HMA overlay on US 59 during the 7-years' service life that performance was monitored.

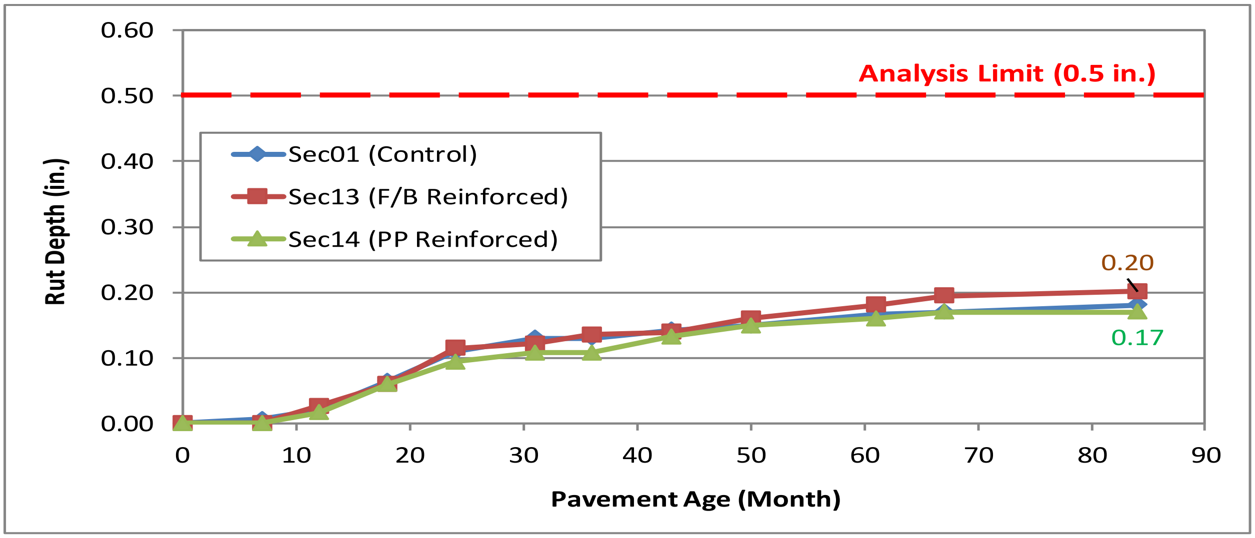

Fig. 6. Pavement Surface Rutting.

Reflective Cracking Performance

As theoretically expected, the un-reinforced Control section (Sec01) exhibited more reflective cracking than the grid reinforced test sections, Sec13 and Sec14. After 7 years of service, the reflective cracking on Sec01 is 17% versus 4% for the grid-reinforced sections, i.e., 4.25 times more cracking (Figure 7). In the 7th year, Fig. 7 shows that about 4.25 times more cracks had reflected thru to the pavement surface on the Control section (Sec01= 17%) than on grid-reinforced sections (Sec13 and Sec14 = 4%), clearly illustrating that the grid reinforcements have mitigated/retarded the reflective-crack propagation.

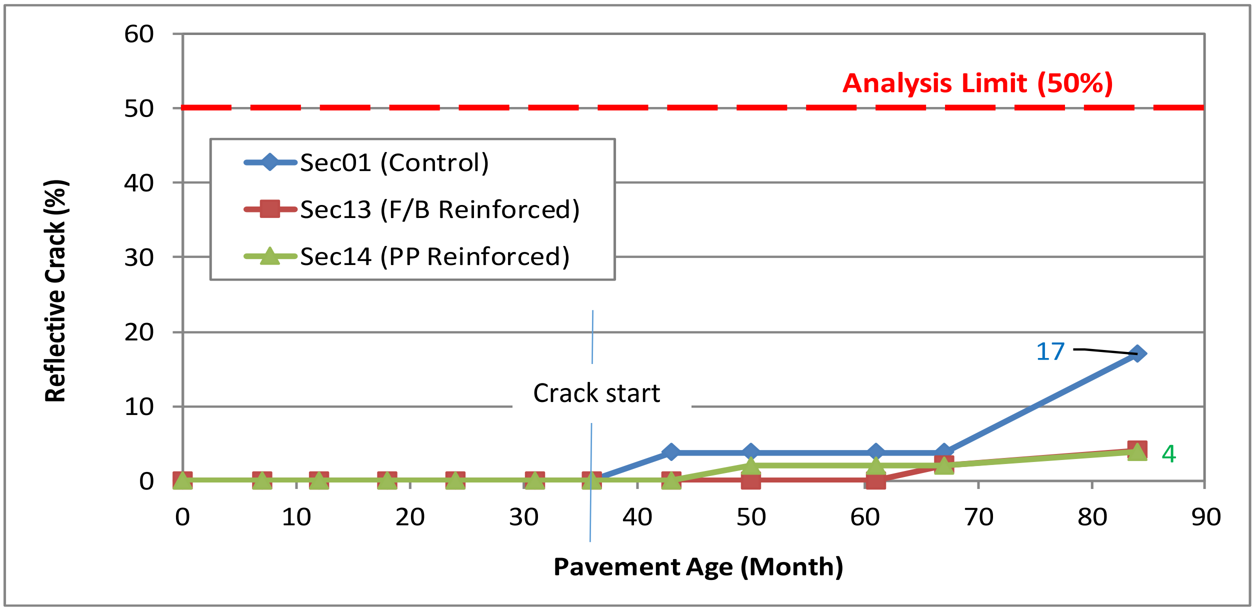

Fig. 7. Reflective Cracking on the Pavement Surface.

Fig. 7 further shows that reflective cracking on Sec01 started just after 3 years (36 months) of service followed by Sec14 at 3.6 years (43 months) and lastly, Sec13 at 5.1 years (61 months). The cracking on Sec01 seems to have accelerated after the 67th month, from about 4% to 17% in the 84th month. While the percentage of cracking is virtually the same (4%) in the 7th year, cracking on Sec14 (PP) started appearing on the pavement surface about 18 months earlier than on Sec13 (F/B). Overall, the cracking on the test sections is still significantly less than the M-E PDG manual of practice and TxME's 50% terminal threshold to warrant any immediate maintenance/rehab attention. However, from the shape of the graph in Fig. 7 and assuming that the deterioration rate remains the same, Sec01 is theoretically not expected to last five more years prior to reaching the 50% terminal criterion – particularly if a more stringent 25% terminal criterion is considered. Note that in lieu of 50%, some literature also recommends a 25% threshold [9].

Longitudinal Profile Measurements – IRI and PSI

Pavement surface roughness/smoothness (IRI) and serviceability index (PSI) were measured and quantified based on the high-speed profile (longitudinal) measurements. With an IRI of 81 and 74 in/mile for Sec13 and Sec14, respectively, in comparison to Sec01 (Control) with 58 inch/mile, Fig. 8 suggests that the grid reinforcements have an impact on the pavement surface smoothness/roughness, particularly if not well installed. Right from construction and throughout the 7-years' service life, Sec01 (Control) has exhibited a smoother pavement surface with the lowest IRI value, with Sec13 (F/B) being the least at 81 in/mile in the 7th year – all subjected to the same traffic level, climatic conditions, and similar pavement structure. Although all the test sections are still well below FHWA's condition rating criterion of IRI ≤ 170 inch/mile, the results suggest that, for the 7-years' service life evaluated, the PP grid material was a little superior to F/B in terms of providing a smoother pavement surface [9].

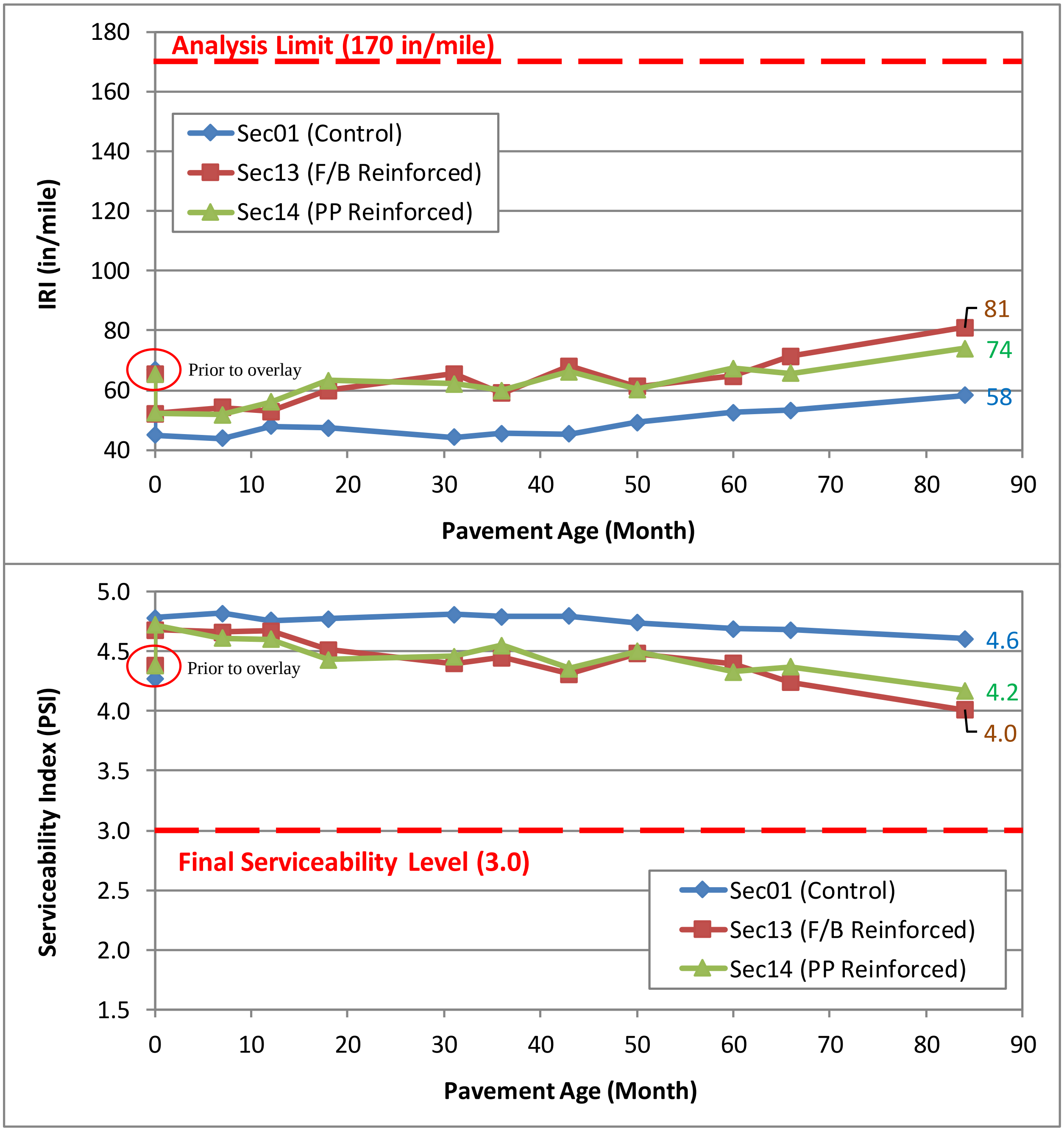

Fig. 8. Pavement Surface Roughness (IRI) and Serviceability Index (PSI).

As evident in Fig. 8, the trend in the PSI results is similar to that of the IRI results, with Sec01 (Control) exhibiting superior performance, i.e., highest PSI values, in fact, 4.6 in the 7th year of service. For the grid-reinforced sections, Sec14 (PP) is slightly better than Sec13 (F/B), i.e., 4.2 versus 4.0. Using PSI ≥ 3.0 as the tentative terminal threshold based on the Texas pavement manual, the PSI performance is thus far rated as satisfactory on all the test sections [9]. Note however that the grid-reinforced sections started with higher initial IRI and lower initial PSI values than the Control section right from construction at month zero. By and large, the rate of deterioration (when considering the slopes of the IRI and PSI plots in Fig. 8) on all the three test sections, seems to be hardly different, albeit that the grid-reinforced sections have high IRI and lower PSI values, respectively. However, it is apparent from Fig. 8 that the higher IRI (and lower PSI values) of the two grid-reinforced test sections seems to have started right from the time of construction and therefore, could be mostly construction related, e.g., grid installation, HMA placement, compaction issues, etc. This disparity in the initial IRI and PSI values at the time of construction appears to have continued throughout the service life of the test sections, and, hence, while deteriorating at nearly the same rate, they are performing poorer than the Control section in terms of the IRI and PSI magnitudes. For instance, minor dips (0.25 ft. width and 0.15 in. depth) were measured on the grid-reinforced test sections (during QC/QA profile measurements just after construction) while no noticeable dips or dumps were measured/observed on the Control section. So, these dips may have likely contributed to the higher initial IRI and lower initial PSI values of the grid-reinforced sections as shown in Fig. 8.

It should also be noted that although, in theory, one expects grid materials to be smooth, in reality, this may not always be the case, and in fact, the grid might introduce some minor irregularities to the pavement surface (short wavelength) as evident in this case study (Fig. 8). In the end, it's all about a balance between the benefits gained in terms of reflective crack resistance versus any losses in smoothness. In this case study, however, the minor disparity and increase in pavement surface roughness due to grid-reinforcement is insignificant compared to the superior performance gained in terms of reflective crack resistance shown previously in Fig. 7. As shown in Fig. 9, a plot of the IRI versus PSI was also generated to establish a correlation between these two parameters.

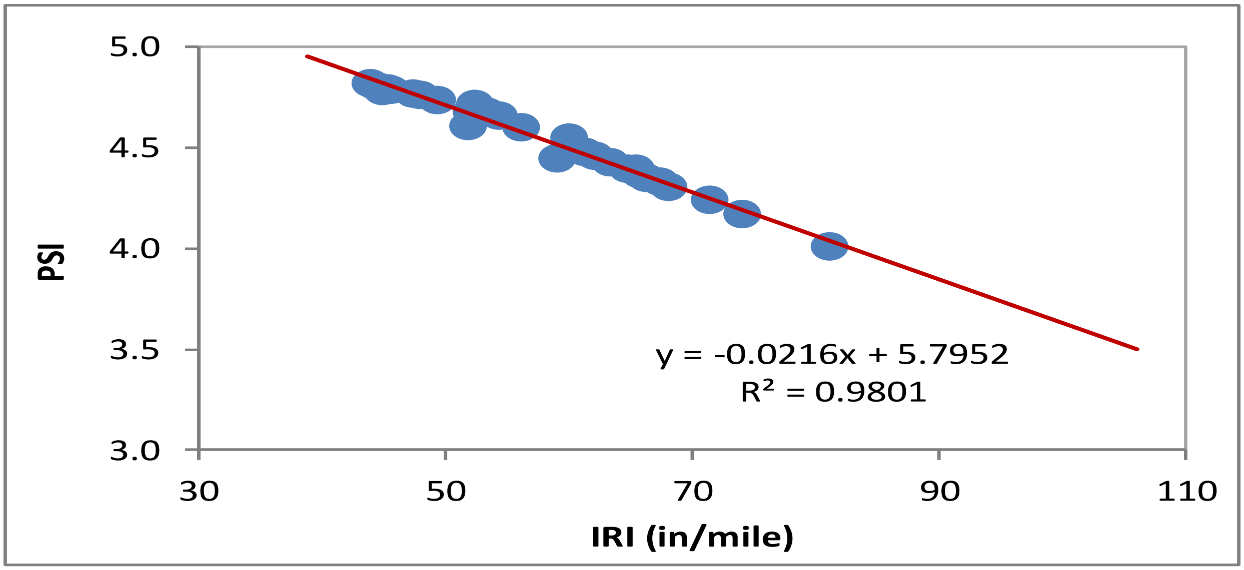

Fig. 9. Graphical Plot of the PSI-IRI Linear Relationship.

At a correlation coefficient of 98% (i.e., R^2 = 0.98), Fig. 9 shows an inverse proportional relationship between IRI and PSI with a regression model of the following linear format:

$$PSI = -a(IRI) + b \qquad \text{(Equation 1)}$$

Where a and b are regression constants 0.0216 and 5.7952. Mathematically, the graphical illustration in Fig. 9 and Equation 1 indicates that as the IRI increases, the PSI correspondingly decreases. This allows for computing one parameter if one of them is known, i.e., PSI from IRI and vice versa. For example, using Equation 1, TxDOT's IRI threshold value corresponding to a PSI = 3.0 would be 129.40 in/mile. And similarly, FHWA's PSI corresponding to IRI = 170 in/mile would be 2.12.

Coring and Interlayer Bonding Evaluation

Field cores were extracted from both the inside and outside wheel paths after over 5 years of service life. As evident in Fig. 10, it was visually observed that all Control and grid-reinforced cores were intact and fully bonded at the layer interface. In the laboratory, the measured interlayer shear-bond strengths, conducted in the shear-bond test at room temperature under a monotonic shear loading rate of 0.2 in/min [15], for all the cores (both Control and grid-reinforced) were all well above 100 psi, averaging 115 psi. The measured interlayer shear-bond strengths were 117 psi (Sec01), 113 psi (Sec13), and 115 psi (Sec14).

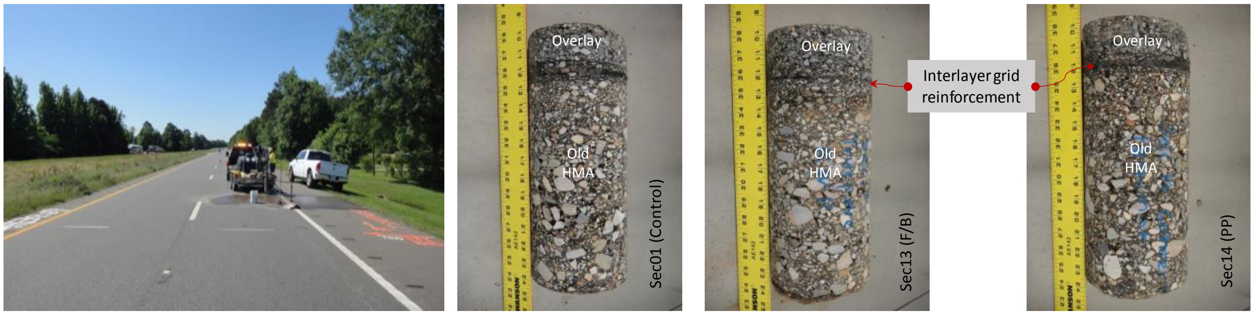

Fig. 10. Intact and Fully Bonded Cores.

Assuming a tentative threshold of 40 psi as proposed by Wilson et al., the measured shear-bond bond strength values (averaging 115 psi) are satisfactory [15,17]. However, even if a tighter threshold value of 100 psi, as proposed by Johnson et al. and Mohammad et al., was considered, all the cores would still pass [18,20]. Furthermore, the measured core shear-bond strength values are indifferent to the reviewed literature range of 15 psi to 217 psi, mostly for un-reinforced HMA [15-29]. Overall, these visual core observations (Fig. 10) and shear-bond strength results suggest that with good construction practices and QA/QC monitoring/testing, there is hardly any adverse effect on the interlayer bond strength due to grid reinforcement.

Pavement Surface View, Surface Texture, and Forensic Evaluations

The pictures in Fig. 11 visually shows surface cracking on Sec01 (Control) with little to none on the grid-reinforced test sections as of April 25, 2018. This is in agreement with Fig. 7 that showed 17% cracking for Sec01 and 4% on Sec13 and Sec14.

Fig. 11. Pictorial Surface View of the US 59 Test Sections.

As seen in Fig. 11, no other defects are visible on the test sections except for the cracking on Sec01. From both coring (Fig. 10) and GPR measurements, no subsurface or forensic defects such as moisture intrusion or localized voiding have been observed on all the test sections as of April 25, 2018. Similarly, the DFT-CTMeter tests also indicated good surface texture and adequate friction characteristics, with the measured speed constant (S_p) and international friction index (IFI) averaging 75.3 and 0.27, respectively, on all the three test sections (ASTM E 1960) [30,31].

DISCUSSION AND SYNTHESIS OF THE FIELD TEST RESULTS

For the same traffic level, climatic conditions, and pavement structure, this field case study indicated that the grid reinforcement materials used on this project, namely paving-mats F/B and PP, had no structural impact on the rutting performance of the HMA overlay. The surface rutting measured during the 7 years performance period was virtually the same on all the three test sections, averaging 0.18 inches after 7 years of service life. Even after enduring the 2,612 daily 18-kip ESALs and the high Texas summer temperatures (ambient), often exceeding 100°F for a 7-year service period, the surface rutting on the three test sections is way below the 0.5-inches terminal threshold, with a measured maximum rut depth of 0.2 inches for Sec13 (F/B grid-reinforced). This good rutting-resistance performance is partially attributed to the good pavement structural strength (stiffness/modulus) and good QA/QC construction practices. Note that the average measured FWD and DCP moduli for the US 59 pavement structure at 77 °F were: HMA overlay = 423 ksi, existing HMA = 490, base = 130 ksi, and subgrade = 44 ksi [9,32]. Considering the shape and slopes of the three rutting curves in Fig. 6, it still theoretically remains to be seen if the results will be any different from the excellent performance trend reported in this paper after 7 years of service life.

With respect to reflective cracking, the field performance is as theoretically expected. While still significantly below the 50% terminal threshold value after 7 years of service life, Sec01 (Control), at 17% of reflective cracking, has already cracked 4.25 times more than the grid-reinforced sections (Sec13 and Sec 14) whose cracking has only reflected by about 4.0% to the surface. In fact, cracking on Sec13 (F/B grid-reinforced) started reflecting and appearing on the pavement surface about 25 months after cracking had already initiated on Sec01 (Control). However, if a more stringent 25% terminal criterion is used, Sec01 (Control), would be considered almost failing having exhausted 68% (i.e., 17% of 25%) of its reflective crack life versus only 16% (i.e., 4% of 25%) for grid reinforced sections [9]. This evidently proves the potential performance benefits of using grid reinforcements in HMA overlay to mitigate reflective cracking.

Based on the traffic benefit ratio (TBR) concept from AASHTO R 50-09 [33], the GEF equivalency concept was adopted in this study to evaluate and quantify the potential field cracking resistance improvements and performance benefits of using grid reinforcements in HMA overlay construction. In this paper, the GEF was arbitrarily formulated and determined as a composite function of the following three variables using the Control section as the reference datum: (a) time taken for the existing crack to propagate and start reflecting on the pavement surface; (b) rate of crack growth from the time of the first crack initiation up to N^{th} year of service life; and (c) percentage surface cracking in the N^{th} year of service life. The GEF formulation is expressed in Equations 2 and 3:

$$GEF = R_C\left(\frac{(\%Cracking\ on\ C_N)}{(\%Cracking\ on\ X_N)}\right)\left(\frac{T_X}{T_C}\right) \qquad \text{(Equation 2)}$$

$$R_C = 1 - \left(\frac{Cr_i}{Cr_C}\right) \qquad \text{(Equation 3)}$$

In Equation 2, GEF = grid efficiency factor, $\%Cracking\ on\ C_N$ and $\%Cracking\ on\ X_N$ are the percentage surface cracking on the Control section and test section X, respectively, in year N (7 years in this case); T_C and T_X is the time cracking started on the Control and test section X, respectively. In Equation 3, R_c is the normalized crack growth-rate factor; and Cr_i and Cr_C are the crack growth rate on the Control and test section *i*, respectively, which is essentially the graph slope of the percentage crack-time plot from the time of the first crack start, i.e., 36 months in Fig. 7.

As evident in Fig. 7, the percentage cracking in the 7th year on Sec13 and Sec14 are the same (4%). However, the crack start time and crack growth rates (slope of the graphs) are different. Similarly, starting to crack earlier or later, does not automatically translate into more cracking on a test section. This is the reason GEF (Equation 2) was formulated and computed as a composite function of these three variables, namely, crack start time, crack growth-rate factor, and percentage cracking, in this paper. Using Fig. 7 and Equation 2, the computed GEF results are listed in Table 2.

Table 2 GEF Results.

Test Section	Cracking Ratio @ 7 years	Crack Start Time (T_i) Ratio	Normalized Crack Growth-Rate Factor (Rc)	GEF
Sec01 (Control)	1.00	1.00	1.00	1.00
Sec13 (F/B)	(17%/4%) = 4.25	(61/36) =1.69	0.62	4.43
Sec14 (PP)	(17%/4%) =4.25	(43/36) = 1.19	0.81	4.11

In Table 2, Sec01 (Control) is the reference datum and thus, all the data variables have been arbitrarily assigned a value of 1.00. Although the 7th year percentage cracking on Sec13 and Sec14 are the same (Fig. 7) with a *crack ratio* of 4.25, the computed performance benefit of each grid-reinforcement material in Table 2, expressed in terms of GEF, are slightly differently 4.43 and 4.11 for F/B and PP, respectively. As expressed in Equation 1, this is attributed to the differences in the *crack start time* (T_i) and *crack growth-rate factor* (R_c). For instance, while cracking started to manifest only in the 61st month on Sec13 (versus 43rd month for Sec14), the crack growth rate (slope of the %cracking-time plot in Fig. 7) was higher than that on Sec13. Thus, resulting in a relatively lower crack growth-rate factor (0.62 [Sec13] versus 0.81 [Sec14]) but vice versa for the crack start-time ratio (i.e., 1.69 [Sec13] versus 1.19 [Sec14]).

In general, the results in Table 2, based on a 7-year service life, show that the two grid materials (paving-mats) are statistically indifferent and will yield performance benefits on the order of about 4.43 (F/B) and 4.11 (PP) times more than an un-reinforced HMA overlay in terms of reflective crack-resistance and overlay longevity. However, based on F/B's high crack growth rate after the 61st month of service as depicted in Fig. 7, there is a theoretical expectation that Sec13 (F/B) might deteriorate at a faster rate and reach the 50% terminal criterion earlier than Sec14 (PP) for a performance period exceeding 7 years. This is more so, especially considering that fiberglass, which is an elemental component of the Sec13 grid material (Fig. 2), is generally more brittle than the polypropylene-based material making up the Sec14 grid material. Overall, the computed GEF values in Table 2 are satisfactorily comparable and insignificantly different from the reviewed literature range of 1.1 to 6.0 [2,5,7,15].

Other performance indices evaluated and discussed in this paper included the pavement surface smoothness/roughness, serviceability, and interlayer bonding conditions. In terms of pavement surface smoothness and serviceability, the Control section outperformed the grid-reinforced test sections by about 34% and 12% for the IRI and PSI, respectively. The measured IRI values in the 7th year of service were 58 in/mi (Sec 01), 81 in/mi (Sec13), and 74 in/mi (Sec 14), respectively; while it was 4.6 (Sec 01), 4.0 (Sec13), and 4.2 (Sec14) for the PSI, respectively (Figure 8). Considering that the difference in the IRI-PSI magnitude/performance started right from QC/QA profile measurements just after construction, while the deterioration rate is hardly different from the Control test section, the higher IRI and lower PSI values (initial) are most likely construction related, i.e., grid installation, HMA placement, compaction, etc. That is the grid-reinforced sections already started with higher initial IRI and lower initial PSI values than the Control section right from construction at month zero.

On a comparative note, Sec14 (PP) outperformed Sec13 (F/B) in terms of both the IRI (9%) and PSI (5%), i.e., presenting a relatively smoother pavement surface with better ride quality than Sec13. Overall, although both the computed *IRI* (≤ 170 in/mi) and *PSI* (≥3.0) indices are still way below their respective terminal thresholds, the results presented in this paper infers that grid-reinforcement may have adverse impacts on the pavement surface condition if not well installed during HMA overlay construction. Thus, proper grid installation, construction, and good QA/QC practices are imperative to minimize these effects.

Like for rutting performance, the grid reinforcements exhibited no major bearing on the pavement surface texture and friction characteristics during the 7-year performance period. As of April 25, 2018, all the three test sections indicated fair surface/friction characteristics with the same level of IFI, averaging about 0.27. Nonetheless, field monitoring is still ongoing to comparatively assess performance beyond 7 years.

As previously shown in Fig. 10, cores extracted from both the Control and grid-reinforced test sections were all in an intact condition. The laboratory measured interlay shear-bond strength on the cores averaged over 100 psi, well above the 40 psi tentative threshold criterion and satisfactorily comparable to the reviewed literature range of 15-217 psi [15-29]. Overall, these findings suggest that with good construction practices and stringent QA/QC protocols, an equivalent level of interlayer bonding similar to traditional un-reinforced HMA is attainable with grid-reinforced HMA overlays – as is the case with the grid materials used in this study.

SUMMARY AND RECOMMENDATIONS

This paper presented highway US 59 (in Atlanta District of Texas) as an in-service field case study to share the practical experiences and lessons learned, and demonstrate the performance benefits, merits, and demerits of using grid reinforcements in HMA overlays. Particular emphasis was on reflective crack mitigation, pavement surface roughness/texture, and interlayer bonding. The key findings and recommendations drawn from the study are summarized below:

- For the highway US 59 pavement structure subjected to daily 2,612 18-kip ESALs under the Texas summer temperatures of reaching over 100°F, the grid reinforcement material (F/B and PP) used on this project exhibited no structural bearing or negative effects on the rutting performance of the HMA overlay. The surface rutting measured on all the three test sections averaged 0.18 inches after 7 years of service life - way satisfactorily below the 0.50-inch terminal threshold value.

- As theoretically expected, the grid-reinforced test sections outperformed the Control section in terms of reflective crack-resistance performance. Although well below the 50% terminal threshold criterion, the reflective cracking was 17% on the Control section versus 4% on the grid-reinforced test sections after 7 years of service life.

- Computed as a function of the crack start-time, crack growth (slope of the %crack-time plot), and percentage surface cracking in year 7, the GEF values were determined to be 4.43 and 4.11 for the F/B and PP grid materials, respectively, which are indifferent from the reviewed literate range of 1.1-6.0. For the pavement structure, materials, traffic loading, and climatic conditions in question, this infers that the performance benefit of using these grid reinforcement materials in terms of reflective crack-resistance and overlay longevity is over four times better than an un-reinforced HMA overlay.

- In terms of pavement smoothness and serviceability indices, the Control section outperformed the grid-reinforced test sections with a lower IRI (i.e., 34% better) and higher PSI (i.e., 12% better) value, respectively. The measured IRI was 58 in/mi (Control) and 71 in/mi (grid-reinforced) with

PSI as 4.6 (Control) and 4.1 (grid-reinforced). In terms of grid material comparison, PP (Sec 14) outperformed F/B (Sec 13). Although both the measured IRI (≤ 170 in/mi) and PSI (≥3.0) values were satisfactorily below their respective terminal criterion, the results and findings suggests that grid-reinforcement may have an impact on the pavement surface condition and thus, proper care needs to be taken during grid installation and HMA overlay construction to mitigate these effects.

- With good construction practices and stringent QA/QC protocols, an equivalent level of interlayer bonding similar to traditional un-reinforced HMA is attainable with grid-reinforced HMA overlays. In this study, a similar level of interlayer bonding with an interlayer shear-bond strength averaging over 100 psi was measured on intact cores extracted from both the Control and grid-reinforced test sections, after over 5 years of service life. That is, with good construction practices and QA/QC protocols, the same level of interlayer bonding is achievable whether the HMA overlay is grid-reinforced or not.

Overall, the study results have demonstrated the performance benefits and impacts of using grid-reinforcement in HMA overlays, using highway US 59 in the Atlanta District of Texas, as a field case study. As part of the Texas pavements database (DSS) project, performance monitoring on the test sections is still ongoing and the DSS will keep on being updated and populated with more field performance data. While the grid materials used in this case study exhibited satisfactory reflective crack-resistance performance as theoretically expected, the following are recommended for future studies: (a) conducting a life cycle cost analysis (LCCA) to comparatively quantify the economic benefits of the grid-reinforcements, (b) developing a standardized methodology for screening and selecting grid materials during the HMA overlay design stage, and (c) devising a standardized interlayer bond strength test procedure and screening criteria for grid reinforcement in HMA.

ACKNOWLEDGEMENTS AND DISCLAIMER

The authors thank TxDOT and the Federal Highway Administration (FHWA) for their financial support and all those who helped during the course of this research work. Special thanks also go to all those who assisted with laboratory testing and fieldwork during the course of this study. In particular, special thanks go to Esra'a Alrashydah for her timely assistance and inputs.

The contents of this paper reflect the views of the authors who are responsible for the facts and accuracy of the data presented herein and do not necessarily reflect the official views or policies of any agency or institute. This paper does not constitute a standard, specification, nor is it intended for design, construction, bidding, contracting, tendering, certification, or permit purposes. Trade names were used solely for information purposes and not for product endorsement or certification.

REFERENCES

[1] A. Khodaii, S. Fallah, F. M. Nejad, Effects of Geosynthetics on Reduction of Reflection Cracking in Asphalt Overlays. Geotextiles and Geomembranes. 27(1), (2009), 1–8. doi: 10.1016/j.geotexmem.2008.05.007
[2] AG (2013). Alliance Goesynthetics – Pavement Interlayer System. Technical Brochure, NILEX Civil Environmental Group, USA.
[3] G.S, Cleveland, J.W. Button, R.L. Lytton, Geosynthetics in Flexible and Rigid Pavement Overlay Systems to Reduce Reflection Cracking. Research Report# FHWA/TX-02/1777. (2002), PP 1-297. Texas Department of Transportation (TxDOT) - RTI, TX, USA.
[4] Thin Bituminous Surfacing Systems. Agrément South Africa (ASA).

[5] R. Fyfe, Geotextile Reinforced Seals under Asphalt. Paper Publication. Geofabrics Australasia, (2011), Australia.

[6] M. Elseifi, R. Bandaru, Cost Effective Prevention of Reflective Cracking of Composite Pavement. Research Report FHWA/LA.11/478. LSU, (2011), Baton Rouge, USA.

[7] TI (2015). Tensar International. GlasGrid Pavement Reinforcement System - The GlasGrid® System Extends Pavement Life thus Reducing Maintenance and Life Cycle Costs. GlassGrid Brochure, USA.

[8] L.F. Walubita, A.N. Faruk, J. Zhang, X. Hu, Characterizing the Cracking and Fracture Properties of Geosynthetic Interlayer Reinforced HMA Samples using the Overlay Tester (OT), Constr. Build. Mater. 93 (2015) 695 - 702. doi.org/10.1016/j.conbuildmat.2015.06.028.

[9] L.F. Walubita, S.I. Lee, A.N. Faruk, T. Scullion, S. Nazarian, I. Abdallah, Texas Flexible Pavements and Overlays: Year 5 Report—Complete Data Documentation (No. FHWA/TX-15/0-6658-3), (2017). Texas A&M Transportation Institute.

[10] J.G.Zornberg, Advances in the Use of Geosynthetics in Pavement Design. Conference Proceedings. Geosynthetics India'11, IIT Madras, Chennai, Sept 23-24, 2011.

[11] Colbond (1998). TRC-Grid, Design and Installation Guide. Akzo Nobel Geosynthetics, Arnhem, The Netherlands, 24p.

[12] H. Siriwardane, R. Gondle, B. Kutuk, Analysis of Flexible Pavements Reinforced with Geogrids, Geotech Geol Eng (2010) 28: 287. https://doi.org/10.1007/s10706-008-9241-0.

[13] B.G.J. Uijting, C.G. Jenner, A.J.T. Gilchrist, Evaluation of 20 years experience with asphalt reinforcement using geogrids, Proceedings of the 3rd International Conference On Bituminous Mixtures and Pavements, 2002, 869-877.

[14] W.-L, Zou, Z. Wang, H.-M. Zhang, Field trial for asphalt pavements reinforced with geosynthetics and behavior of glass-fiber grids, Journal of Performance of Constructed Facilities, 21, 2007, 361-367

[15] L.F. Walubita, T.P. Nyamuhokya, J.J. Komba, H.A. Tanvir, M.I. Souliman, B. Naik, Comparative assessment of the interlayer shear-bond strength of geogrid reinforcements in hot-mix asphalt, Constr. Build. Mater. 191 (2018) 726-735. doi.org/10.1016/j.conbuildmat.2018.10.035.

[16] J.P. Zaniewski, S.F. Knihtila, H.N. Rashidi, Evaluation of the Bond Strength of Asphalt Overlay. Proceedings of International Airfield & Highway Pavements Conference 2015.

[17] B. Wilson, A. Seo, M. Sakhaeifar, Performance Evaluation and Specification of Trackless Tack. FHWA/TX-16/0-6814-1. Texas Transportation Institute, College Station, TX, 2013.

[18] E. Johnson, N. Cruz, T. Wood, Using the Florida Bond Test to Improve HMA Bond Strength and Durability – Technical Summary Report. MN, USA, 2015.

[19] L. Mohammad, M. Elseifi, A. Bae, N. Patel, NCHRP Report 712: Optimizing Tack Coat for HMA Placement. Washington DC – The National Academies Press, 2012.

[20] N.H. Tran, R. Willis, G. Julian, Refinement Of The Bond Strength Procedure And Investigation Of A Specification. NCAT Report # 12-04. Auburn, AL, 2012.

[21] M. Solaimanian, (2013). Paving the Way. APA, Harrisburg, PA.

[22] PI-Pavement Interaction: http://www.pavementinteractive.org/article/de-bonding-of-hma-pavementslayer-bonding-2/ Accessed July2017.

[23] Gharaybeh et al. (2010). Evaluation of Bond Strength Between Old and New Pavement Overlays. Paper extract from Maters Thesis. JUST, Irbid, Jordan.

[24] O. Vacin, J. Ponniah, S. Tighe, Quantifying the shear strength at the asphalt interface. Proceeding of the 1st Annual International university Symposium on Infrastructure Management (AISIM); 2005 Aug; University of Waterloo, Waterloo, Canada.

[25] E. Denneman, W.J. vdM. Steyn, A.T. Visser, Guidelines for the Assessment and Certification of Thin Bituminous Surfacing Systems. Agrément South Africa (ASA).

[26] G. White, Asphalt Overlay Bond Strength. Conference Proceeding - Airfield Pavement and Lighting Forum, At Sydney, New South Wales, Australia, 2015.

[27] H. Wang, Z. Wang, T. Bennert, R. Weed, HMA Pay Adjustment. Report# FHWA NJ-2015-007, Piscataway, NJ, 2015.

[28] K.K. McGhee, T. Clark, Bond Expectations for Milled Surfaces and Typical Tack Coat Materials Used in Virginia. Research Report# 09-R21. VTRC, VA, 2009.
[29] R.C. West, J. Zhang, J. Moore. Evaluation of Bond Strength between Pavement Layers. NCAT Report 05-08. National Center for Asphalt Technology, Auburn, AL, 2005.
[30] ASTM (2018). Annual Book of ASTM Standards, West Conshohocken, PA, USA.
[31] L. Fuentes, M. Gunaratne, Revised Methodology for Computing the International Friction Index (IFI). Transp Res Record 2011; 2227: 129-137.
[32] X. Hu, A.N. Faruk, J. Zhang, M.I. Souliman, L.F. Walubita, Effects of tire inclination (turning traffic) and dynamic loading on the pavement stress–strain responses using 3-D finite element modeling. International Journal of Pavement Research and Technology, 10(4), 2017, 304-314.
[33] AASHTO (2013). AASHTO Designation R 50-09 (2013). Standard Practice for Geosynthetic Reinforcement of the Aggregate Base Course of Flexible Pavement Structures. Washington DC, USA.